ELSEVIER

Surface Science 448 (2000) 269–278

surface science

www.elsevier.nl/locate/susc

LEED investigations on Co(0001): the $(\sqrt{3}\times\sqrt{3})$R30°-CO overlayer

J. Lahtinen [a,b,*], J. Vaari [a,1], K. Kauraala [a], E.A. Soares [b], M.A. Van Hove [b,c]

[a] *Laboratory of Physics, Helsinki University of Technology, P.O. Box 1100, 02015 Helsinki, Finland*
[b] *Materials Sciences Division, Lawrence Berkeley National Laboratory, University of California, Berkeley, CA 94720, USA*
[c] *Department of Physics, University of California, Davis, CA 95616, USA*

Received 18 September 1999; accepted for publication 7 December 1999

Abstract

The local adsorption structure of CO on Co(0001) has been determined at 160 K using dynamical low-energy electron diffraction (LEED). The CO molecules in the $(\sqrt{3}\times\sqrt{3})$R30°-CO overlayer adopt the on-top site with the CO axis perpendicular to the surface and induce buckling in the top Co layer pulling the Co atom beneath the CO by 0.04 ± 0.04 Å outwards. The optimum length for the CO bond is 1.17 ± 0.06 Å and that for the C—Co distance 1.78 ± 0.06 Å. The first-layer Co—Co distance is 2.04 Å and thus only slightly expanded from the bulk value. The structure obtained is compared with other known CO structures on transition metals.

Keywords: Carbon monoxide; Cobalt; Low energy electron diffraction (LEED); Surface structure, morphology, roughness, and topography

1. Introduction

The adsorption of CO on transition metal surfaces has been extensively studied for over 20 years with the aim of understanding the chemical bond of CO to the surface. A large fraction of the studies have been performed on Ni, and many other transition metals have received their share of the interest, but studies on cobalt surfaces have been relative rare compared with its neighbors in the Periodic Table despite the importance of cobalt as a catalyst material for certain reactions. The database of structural analyses [1] indicates that the adsorption structures of CO have been published on the closed-packed surfaces of Ru [2,3], Rh [4], Pd [5,6], Pt [7], Ni [8], and Cu [9], all of them, save Pt, exhibiting a $(\sqrt{3}\times\sqrt{3})$R30° structure. The adsorption site for CO is on top in most cases but on Ni(111) bridge sites [8] and on Pd(111) fcc-hollow sites [5,6] have been observed. The adsorption of CO on Co(0001) has been studied in the past with e.g. thermal desorption spectroscopy (TDS) [10,11], work function measurements [11,12], low-energy electron diffraction (LEED) [10–13], and photoemission spectroscopy [12,13]. Based on these studies we know that the adsorption takes place molecularly on the surface and three ordered structures are formed: for low coverages ($\theta<0.33$) a $(\sqrt{3}\times\sqrt{3})$R30°, in a narrow coverage range $0.33<\theta<0.45$ a $(\sqrt{7/3}\times\sqrt{7/3})$R10.9°, and below the saturation coverage $\theta<0.67$

* Corresponding author. Fax: +358-9-451-3113.
E-mail address: jouko.lahtinen@hut.fi (J. Lahtinen)
[1] Present address: VTT Building Technology, Fire Technology, P.O. Box 1803, 02044 VTT, Finland.

0039-6028/00/$ - see front matter
PII: S0039-6028(99)01228-5

a $(2\sqrt{3}\times 2\sqrt{3})$R30°-7CO [10–13]. In the $(\sqrt{3}\times\sqrt{3})$R30° structure, the CO molecules have been claimed to reside on the top site perpendicular to the surface based on valence band [13] and core level measurements [11]. Cobalt is located in the Periodic Table at the border of the molecular adsorption for CO [14] with its neighbors Ni and Fe clearly contrasted in their ability to dissociate CO. At room temperature, the adsorption on Ni is molecular and that on Fe is dissociative. On defect-free Co(0001) and Co(10$\bar{1}$0) [15] CO does not dissociate but on the more open faces, such as Co(11$\bar{2}$0) [16] and Co(10$\bar{1}$2) [17] as well as on polycrystalline Co [18,19], dissociation of CO has been observed above room temperature as a competing channel for CO desorption. In this respect we will discuss the CO bond lengths and the possible trends for CO dissociation on transition metal surfaces. This work is part of a larger study of adsorbate structures of Co(0001) where the structures of the clean surface and the (2×2)-K overlayer have already been published [20,21], and the existence of the various CO [11] and CO + K coadsorption structures [22] have been reported earlier. In this work we report on the $(\sqrt{3}\times\sqrt{3})$R30° surface structure of CO on Co(0001). The CO molecules adopt the on-top site and the bond lengths obtained for this structure are in line with the previously studied systems.

2. Experimental

The experiments were performed in a stainless steel UHV chamber with facilities for X-ray photoelectron spectroscopy (XPS), Auger electron spectroscopy (AES), low-energy ion scattering (LEIS), thermal desorption spectroscopy and low-energy electron diffraction measurements. The system was pumped with an ion pump, and the base pressure during the experiments was around 50 nPa. A more detailed description of the UHV setup is available elsewhere [22–24].

The Co(0001) sample with a diameter of 11 mm was spot-welded to the sample holder via 0.25 mm tantalum wires, which were used both for resistive heating and conducting heat to the heat sink cooled with liquid nitrogen. This setup resulted in a lowest attainable sample temperature of 160 K, as measured by a K-type thermocouple spot-welded to the sample edge. This temperature was also used in the experiments. The whole manipulator stage could be rotated around the vertical axis and the sample holder could be rotated around the sample normal providing azimuthal rotation and accurate alignment of the sample normal along the electron beam. The initial cleaning procedure of the sample has been described earlier [23]. Between the experiments, the surface residues were removed by 1 h sputtering with 1.1 keV Ar^+ ions, followed by annealing at 650 K for 1–2 h.

Cleanness of the sample was checked by measuring the O 1s and C 1s peaks using XPS. The final test for the cleanliness is the formation of the LEED pattern of the $(\sqrt{3}\times\sqrt{3})$R30° structure. This surface structure was obtained by exposing the Co(0001) crystal to 1.25 L of CO at 160 K. This exposure was determined by following the quality of the LEED pattern and the TDS yield as a function of CO exposure and it has been reported earlier along with the formation of various surface structures [11].

The LEED experiments were made with a four-grid rear-view LEED unit[2], equipped with a custom made sample biasing and image recording facility. The diffraction images were recorded with a black-and-white video camera connected to a video grabber card on a computer. One video frame had a resolution of 512×512 pixels of 256 grayscales. The same computer was used to drive the LEED controller unit, allowing automated measurements of the intensity versus voltage curves.

The study of the adsorption structures of CO with electron diffraction faces a common problem on most surfaces. The electron beam destroys the ordered layer by either stimulating CO desorption or inducing CO dissociation. In order to extend the length of the LEED measurements on a fragile surface, the exposure of the electron beam is normally reduced by decreasing the beam current to a minimum level still enabling the measurement.

[2] PRI 8-150 RVL 8-120 M2 model LEED unit controlled with PHI 11-020 LEED electronics.

Several additional ways to avoid the problem have been reported in the literature: dividing the measurement in smaller fractions and combining the data [2], recording of the video signal and digitizing it after the measurement [6], or deflecting the electron beam away from the sample using a collector electrode at high potential to attract the electrons during standby time of the measurement [25]. We have constructed a computer-controlled sample bias system that can be used to bias the sample to a high negative voltage to repel electrons while the beam energy is changed and data transferred from the video camera to the computer. The bias voltage can be rapidly removed using a fast MOSFET switch before the LEED images are recorded.

The degree of damage due to the electron beam was estimated by comparing visually the spot sizes and the brightness of the background before and after the LEED measurement. If the quality of the LEED pattern was decreased during the measurement, the data was not used in the I–V analysis. The spot intensities in the diffraction images were analyzed off line after the measurement with home-made software producing the experimental $I(E)$ (intensity versus energy) curves. The shape of the measured spot area is circular and its size is adjusted to give a constant area in the k-space.

3. Computational details

The theoretical $I(E)$ spectra were calculated using the Symmetrized Automated Tensor LEED package of Barbieri and Van Hove [26]. The phase shifts were calculated using the Barbieri/Van Hove phase shift package [26]. We used nine phase shifts and up to 55 symmetrically inequivalent beams in the calculation. The use of nine phase shifts was estimated to be sufficient because both C and O are light scatterers. Also, in some previous calculations a higher number of phase shifts has been used with no decrease in the R factor. The real part of the inner potential was varied in the R factor analysis. The imaginary part of the inner potential had a constant value that was fitted manually along the other parameters. The step size for varying the structural parameters was 0.05 Å and it was further decreased down to 0.01 Å in the final analysis. For the substrate Co layers a Debye temperature of 385 K was used. For the outermost Co layer an enhanced vibration amplitude was used, being $\sqrt{2}$ times the root mean square amplitude in the substrate. The Debye temperatures of the C and O atoms were originally set at 400 K [3]. The rumpled substrate layers were treated as composite layers, and the calculation of the scattering matrices was performed using matrix inversion. The scattering between the layers was accomplished by renormalized forward scattering.

Theoretical and experimental $I(E)$ spectra were compared using the Pendry R factor [27]. The total energy range of the symmetrically inequivalent beams was 1380 eV, of which 680 eV was for integer-order beams and 700 eV for fractional-order beams. Because of two possible terminations of the surface, both exhibiting threefold symmetry, the diffraction pattern has sixfold symmetry and thus each experimental curve can be calculated as an average of six individual spots. In the calculations both terminations have threefold symmetry but they are averaged using equal weight in order to reproduce the experimental data. After obtaining the best-fit structure, the geometric parameters were varied one at a time in the neighborhood of the R factor minimum and the uncertainties of the parameters were obtained using the variance of the R factor.

4. Results

The experimental intensity versus energy curves for the three integer- and three fractional-order beams are shown in Fig. 1 by solid lines. The calculations were started by testing all high symmetry sites for the CO molecule in the adlayer in a rough search. In each reference structure the substrate was ideally terminated. The CO bond length was 1.13 Å and the distance from the C atom to the first Co layer was varied between 1.7 and 1.9 Å. The reference structures were optimized with respect to the atomic positions of the CO

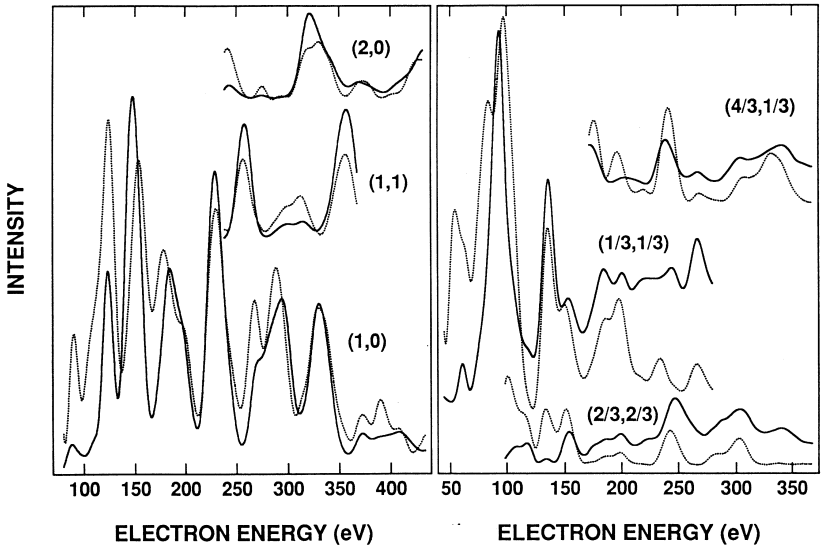

Fig. 1. Experimental (solid lines) and calculated (dashed lines) $I(E)$ curves for the integer-order and fractional-order beams from the $(\sqrt{3}\times\sqrt{3})$R30°-CO structure on the Co(0001) surface.

molecule, two Co layers, and the inner potential. The full data set of three integer- and three fractional-order beams was used for the optimization. The Pendry R factors for the optimized structures after the rough search are summarized in Table 1 together with the R factors for the individual beams. The quality of the fit, as given by the Pendry R factor of 0.359, is moderate. The different adsorption sites were tested also with Zanazzi–Jona R factors and the results indicate top site adsorption with R_{ZJ} values of 0.210 (top), 0.306 (bridge), 0.338 (hcp-hollow) and 0.396 (fcc-hollow).

We also tested the tilting of the CO molecule after the rough search. The results gave a local minimum with 25° tilt angle that was only visible using the Pendry R factor. The perpendicular adsorption is supported by the UPS data of CO on Co(0001) [13], and LEED studies of CO structures on other transition metals. Summing of all this up convinced us that the CO is standing perpendicular to the surface.

Based on the rough search, we concluded that the CO molecules in the $(\sqrt{3}\times\sqrt{3})$R30°-CO structure adopt the top site on the Co(0001) surface with a C—Co distance of 1.77 Å. This structure was then subjected to a refined analysis. A set of reference structures was tested with the CO bond length and the vertical distance between the C atom and the Co atom beneath it independently varied up to $\pm$0.4 Å using several step sizes from 0.05 to 0.01 Å.

Table 1
Pendry R factors for the experimental beams for different high-symmetry adsorption sites for CO on Co(0001)

	(1,0)	(1,1)	(2,0)	(1/3,1/3)	(2/3,2/3)	(4/3,1/3)	R_{tot}
Top	0.290	0.116	0.267	0.461	0.486	0.430	0.359
Bridge	0.387	0.309	0.326	0.496	0.746	0.925	0.539
Hcp	0.422	0.094	0.316	0.782	0.724	0.781	0.542
Fcc	0.355	0.200	0.280	0.725	0.752	0.515	0.503
Final	0.248	0.128	0.223	0.401	0.454	0.456	0.320

The final analysis also included variations of the non-structural parameters. The Debye temperatures of the adsorbed layer were varied between 300 and 700 K. The best fit was obtained with the Debye temperature set at 450 K for both C and O. The imaginary part of the inner potential was varied between -4 and -7 eV, and the best fit was obtained for -5 eV.

The final structure for CO on Co(0001) has a C—O bond length of 1.17 ± 0.06 Å and a C—Co bond length of 1.78 ± 0.06 Å with a Pendry R factor of 0.32 ± 0.05. The best fit values of the R factors of the individual beams are shown on the last line in Table 1. The optimum value of the inner potential is 5.35 eV. The experimental and calculated best-fit intensity versus energy curves for six experimentally available beams are displayed in Fig. 1. The resulting structure of the $(\sqrt{3} \times \sqrt{3})$R30°-CO on Co(0001) surface is presented in Fig. 2 The results also indicate a small buckling of 0.04 ± 0.04 Å in the topmost Co layer, where the Co atom below CO is pulled outwards with respect to the two other surface atoms in the unit cell. The first Co—Co layer distance is 2.04 Å and thus only slightly expanded from the bulk value of 2.034 Å.

5. Discussion

A summary of CO adsorption structures on some transition metals has been given in Table 2. We will comment on the previously deduced structures along with our results below.

The best Pendry R factor of 0.32 obtained for the $(\sqrt{3} \times \sqrt{3})$R30° structure is relatively high for a LEED I–V analysis in general, but reasonable if compared with other CO structures on transition metals. On Pd(111) the $(\sqrt{3} \times \sqrt{3})$R30° structure gave average R factor of 0.30 with a Pendry R factor of 0.55 [6] and on Pt(111) the average R

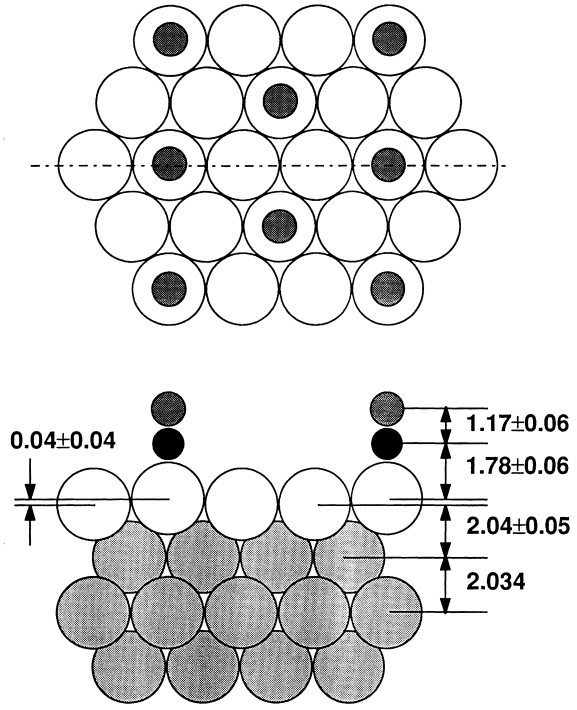

Fig. 2. Top view (upper panel) and side view (lower panel) cut along the [10$\bar{1}$0] direction of the $(\sqrt{3} \times \sqrt{3})$R30°-CO structure on a Co(0001) surface. The white spheres denote the surface Co atoms and the gray spheres the Co atoms of the deeper layers. The small black and gray spheres are carbon and oxygen atoms, respectively. The length unit is 1 Å.

Table 2
Structural results for CO adsorption on transition metal surfaces. A positive value for the buckling means moving the atom beneath the CO molecule outwards. Vib indicates tilted CO molecules with an average tilt angle of zero

Substrate	Structure	θ	T (K)	Site	C−O (Å)	C−substrate (Å)	Buckling (Å)	Tilt angle	Method	Ref.
Co(0001)	$(\sqrt{3}\times\sqrt{3})$R30°	1/3	160	top	1.17±0.06	1.78±0.06	0.04±0.04		LEED	this work
Ru(0001)	$(\sqrt{3}\times\sqrt{3})$R30°	1/3	150	top	1.1±0.1	2.0±0.1			LEED	[2]
Ru(0001)	$(\sqrt{3}\times\sqrt{3})$R30°	1/3	150	top	1.10±0.05	1.93±0.04	0.07±0.03	vib	LEED	[3]
Ni(111)	$(\sqrt{3}\times\sqrt{3})$R30°	1/3	RT	bridge	1.13	1.78±0.05			PED	[8]
Rh(111)	$(\sqrt{3}\times\sqrt{3})$R30°	1/3	240	top	1.20±0.05	1.87±0.04	0.08±0.06	vib	LEED	[4]
Pd(111)	$(\sqrt{3}\times\sqrt{3})$R30°	1/3	300	fcc	1.15±0.05	2.05±0.04	n/a		LEED	[6]
Pd(111)	$(\sqrt{3}\times\sqrt{3})$R30°	1/3	200	fcc	1.25±0.11	2.03±0.04	n/a	0±23°	PED	[5]
Cu(111)	$(\sqrt{3}\times\sqrt{3})$R30°	1/3	80	top	1.13	1.91±0.01			ARPES	[9]
Rh(111)	(2×2)-3CO	3/4	240	top	1.15±0.07	1.84±0.07				
				fcc	1.16±0.07	2.13±0.10				
				hcp	1.18±0.07	2.15±0.10			LEED	[4]
Pd(111)	c(4×2)-2CO	1/2	200	fcc	1.14±0.12	2.06±0.04		0±25°		
				hcp	1.14±0.14	2.10±0.04		0±25°	PED	[5]
Pt(111)	c(4×2)-2CO	1/2	150	top	1.15±0.05	1.85±0.10				
				bridge	1.15±0.05	2.08±0.07			LEED	[7]
Ni(111)	c(4×2)-2CO	1/2	120	fcc	1.22±0.09	1.95±0.06				
				hcp	1.18±0.07	1.92±0.04			PED	[28]
Ni(111)	c(4×2)-2CO	1/2		fcc	1.15±0.10	1.99±0.10				
				hcp	1.18±0.10	1.96±0.10	0.11±0.1		LEED	[29]
Cu(110)	(2×1)	1/2	120	top	1.11±0.05	1.87±0.02	−0.14±0.06			[30]
Ni(110)	(2×1)-2CO	1	125	bridge	1.12±0.12	1.95±0.12		17°	LEED	[31]
Ni(110)	(2×1)-2CO	1	120	bridge	1.15±0.02	1.94±0.04		19°	ARPES	[32]
Ni(110)	(2×1)-2CO	1	130	bridge	1.15±0.10	1.85±0.10		20°	LEED	[33]
Rh(110)	(2×1)-2CO	1	190	bridge	1.13±0.10	1.98±0.10		24°	LEED	[34]
Ni(100)	c(2×2)	1/2	120	top	1.15±0.10	1.71±0.10			LEED	[35]
Ni(100)	c(2×2)	1/2	100	top	1.15±0.10	1.72±0.10			LEED	[36]
Ni(100)	c(2×2)	1/2	100	top	1.13±0.10	1.70±0.10			LEED	[37]
Ni(100)	c(2×2)	1/2	RT	top	1.13±0.10	1.80±0.04			PED	[8]
Cu(100)	c(2×2)	1/2	100	top	1.13	1.92±0.05			NEXAFS	[38]
Cu(100)	c(2×2)	1/2	100	top	1.13±0.10	1.90±0.10			LEED	[35]
Pd(100)	$(2\sqrt{2}\times2\sqrt{2})$R45°-2CO	1/2	350	bridge	1.15±0.10	1.93±0.10			LEED	[39]

factor was 0.29 also accompanied by a higher Pendry R factor [7]. The reason for this may lie in the dynamical tilt of the CO molecule on the surface as found in the case of CO on Ru(0001) [4].

The CO molecule adsorbs at the top site on Co(0001). With similar $(\sqrt{3}\times\sqrt{3})$R30° symmetry on closed packed surfaces the top site is also occupied on Ru(0001) [2,3], Rh(111) [4], and Cu(111) [9]. For Ni(111) CO adsorbs on the bridge site [8] and on Pd(111) on the fcc site [5,6].

It seems that the on top site is a preferred site for CO adsorption on transition metal surfaces at low coverages and the Ni group seems to form the exception. However, IRAS measurements of the Pt(111)+$(\sqrt{3}\times\sqrt{3})$R30°-CO structure have been reported to indicate top site adsorption [40], but on Pt at about one third monolayer coverage the evolution of the LEED pattern after CO exposures is very complicated, and even the ordering of the $(\sqrt{3}\times\sqrt{3})$R30° structure is controversial.

IRAS measurements as a function of sample temperature can be used at low coverages to probe the population of different adsorption sites. If the energy difference between two adsorption sites is of the order of thermal energy, the difference in the adsorption energy can be estimated. For example on Pt(111) the on-top site has 60 meV lower

binding energy for CO than the bridge site and on Ni(100) the binding energy to bridge site is 11 meV lower than to the on-top site [41]. On Ru(0001), an calculated energy difference of 60 meV between the on-top and the threefold hollow-hcp site has been reported [42].

On Pd(111) with the $(\sqrt{3}\times\sqrt{3})R30^\circ$ structure Loffreda et al. [43] have calculated adsorption energies for the different high symmetry adsorption sites using density functional theory (DFT). Their results of -2.01 eV (for fcc), -1.98 eV (hcp), -1.81 eV (bridge), and -1.36 eV (top) indicate a clear preference for the threefold hollow site. On Pd(110) a DFT calculation indicates a difference of 0.59 eV between the on-top and short bridge adsorption sites for the (2×1)p2mg structure [44].

For higher coverages the adsorption site on Rh(111) changes and both the fcc and hcp sites become occupied in addition to the top site [4,45]. Our earlier results indicate that for the $(2\sqrt{3}\times2\sqrt{3})R30^\circ$-7CO structure (with $\theta=7/12$) on Co(0001) a fraction of the CO molecules move to higher coordination sites based on both geometric arguments and on the C 1s and O 1s core level shifts [11].

On other cobalt faces the CO adsorption site has been proposed using vibrational spectroscopies, and for coverages $\theta<0.5$ the top site with CO stretch of 1994 cm^{-1} is claimed to be occupied on Co(10$\bar{1}$0) [15]. On Co(10$\bar{1}$2) the CO stretch is at 1980 cm^{-1} indicating top site adsorption [46] although assignment of an adsorption site based on the vibrational data is uncertain, especially at higher coverages [4,43,47].

The most recent LEED studies with on-top adsorption indicate that the topmost substrate layer exhibits a small buckling with the atom below the CO molecule pulled outwards by 0.07 Å for Ru [3] and by 0.08 Å for Rh [4]. For the fcc and hcp sites such a buckling would be quite unlikely because of the symmetry and for the bridge site it has not been reported. Our value of 0.04 Å for Co(0001) is in line with these results, although the error bars equal the value of the buckling.

The direction of the first layer buckling is opposite to what has been found with K adsorption on Co where the K atoms increase their effective coordination by pushing the surface atoms towards the bulk [21]. In this language it seems that the CO wants to decrease its effective coordination even at the on-top site.

The direction of the buckling can be understood in terms of electrostatic interactions between an electron acceptor, such as a CO molecule (electron donor, such as an alkali atom) and the surface atoms. If we assume that the charge transfer between the electron acceptor (donor) and surface atom takes place locally on the surface, the substrate atom below the adsorbate becomes positively (negatively) charged. The first layer of surface atoms has a small positive (negative) charge and a fraction of the electron density is located outside of the surface. We can thus assume that the outward (inward) buckling is due to the attraction (repulsion) between the individual surface atom and the electron density above the surface.

The value of the first Co—Co layer distance equals the bulk value within the error bars. For the other $(\sqrt{3}\times\sqrt{3})R30^\circ$ structures expansion in the first substrate layer has been seen with Pd(111) (6%) [6] and Rh(111) (1.4%) [4]. In contrast, with Cu(111) no expansion was observed [9], and it was not investigated in a recent study with Pd(111) [5]. The small effect of CO on the layer distance indicates a short screening length in the interaction of CO bonding.

The length of the carbon—cobalt bond was found to be 1.78 ± 0.06 Å and the calculated radius for the carbon atom is 0.53 Å if the diameter of the Co atoms equals their distance in the bulk lattice. This bond length gives a C radius equal to that observed in the $(\sqrt{3}\times\sqrt{3})R30^\circ$ structure on Rh(111) surface [4] and slightly smaller than that on Ru(0001) (0.58 Å) [3]. On Cu(111) the C radius is larger (0.64 Å) [9].

The carbon—substrate distance in various structures and for various systems has been plotted in Fig. 3 as a function of an effective coordination number. This effective coordination is calculated from the expression

$$C_{\mathrm{eff}} = N_{\mathrm{n}} + \frac{N_{\mathrm{nn}}}{12}\frac{N_{\mathrm{s}}}{N_{\mathrm{ads}}}, \tag{1}$$

where N_{n} is the number of surface atoms the CO

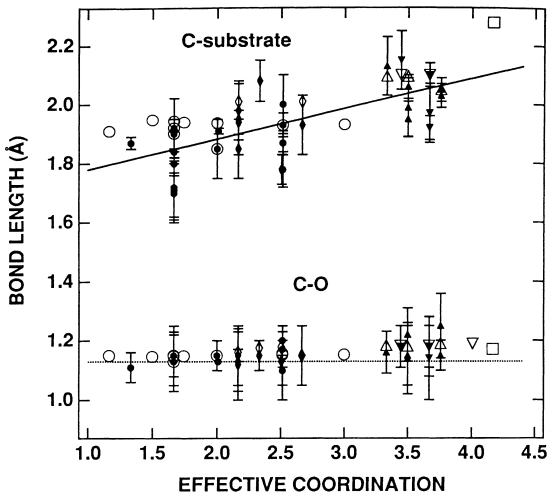

Fig. 3. C—O and C—metal bond lengths as a function of the effective coordination of CO molecules on Co, Ni, Ru, Rh, Pd and Pt surfaces. The different symbols indicate the different adsorption sites as follows: top (○), bridge (◇), fcc (△), hcp (▽), and fourfold hollow (□). The solid symbols represent experimental data and the open symbols calculated values. The solid line is drawn to guide the eye and the dotted line indicates the gas phase value of the C—O bond length. The experimental data have been obtained from references given in Table 2 and the theoretical calculations from Refs. [28,29,42,48,49].

molecule is bonded to as determined by the adsorption site and N_{nn} is the number of the next-nearest surface atoms. The latter is divided by 12 to reduce their effect to a fraction corresponding to the number of nearest neighbors in the closed-packed lattice. N_s is the number of surface atoms, N_{ads} is the number of adsorbed atoms and their ratio is the coverage. The effective coordination calculated in this manner is a measure of how many surface atoms are contributing to the bonding of the adsorbed molecule. All the experimental data shown in Table 2 have been used to create data points for Fig. 3. It should be noted that one structure such as $c(4\times2)$-2CO on fcc(111) could result in two separate data points with equal or different coordination numbers depending on the adsorption site. Experimentally fourfold hollow sites have not been found as a site for CO on any surface but they have been shown to be stable in some cases. From Fig. 3 it is obvious that the increase in the coordination number increases at least the carbon—substrate bond length and also to a smaller degree the C—O bond length, although in this parameter the scatter in the data is of the same order as the overall change.

The data of Fig. 3 also contain calculated C—substrate and C—O bond lengths. Calculated values representing both experimentally verified structures and stable trial structures have been included. On Pt(100) the calculation has been made using full-potential linearized augmented plane wave method (FLAPW) [48] for the $c(2\times2)$ structure. On-top, bridge and fourfold hollow sites have been calculated. The corresponding experimental structures do not exist. The result indicates that the C—substrate bond length increases as the effective coordination increases. On Pd(110) calculations using the local-density approximation of the density functional theory (LDA-DFT) for a $c(4\times2)$p2mg structure gave slightly smaller values for the Pd—C distance than those measured using LEED, but the C—O distance was well within the experimental accuracy [44]. The calculated values are reported only for the on-top site. On Pt(111) for the $c(4\times2)$-2CO structure the lengths for the C—Pt and C—O bonds calculated with LDA-DFT approximation agree well with the experimental values [49]. The calculated values are reported only for the on-top site although the structure contains an equal number of CO atoms in the bridge position. On Pd(111) the adsorption structure has been calculated for three different coverages for $(\sqrt{3}\times\sqrt{3})R30^\circ$, $c(4\times2)$-2CO, and $c(2\times2)$-3CO structures [43]. Although several adsorption sites for CO were used, the C—substrate bond lengths are given only for the experimentally observed adsorption sites and they show an increase in the bond length as a function of coordination.

In a recent computational study of CO on Ru(0001), the C—O bond length was found to decrease and the C—substrate bond to increase with increasing CO coverage [42]. The calculations were performed with the DFT method on (2×2), $(\sqrt{3}\times\sqrt{3})R30^\circ$, (2×1), $(\sqrt{3}\times\sqrt{3})R30^\circ$-2CO, (2×2)-3CO, and (1×1) structures. The adsorption site was assumed to be on top. The results of this study are in line with the other data shown in Fig. 3.

The optimum C—O bond length of the molecule on the Co(0001) surface was found to be 1.17 ± 0.06 Å, which is longer than the bond length of 1.13 Å in the gas phase. This is in line with earlier observations as can be seen in Table 2. Only on Ru(0001) [2,3] for the $(\sqrt{3} \times \sqrt{3})R30^\circ$ structure have CO bond lengths smaller than the gas phase value been observed. For other CO surface structures, the (2×1) structures on Ni(110) [31] and Cu(110) [30] exhibit values smaller than the gas phase value. In the comparison of Table 2 our value can be regarded as long and it can be taken to indicate the tendency of cobalt to dissociate CO. On Ni surfaces the bond length in general seems to be smaller than that on Co(0001) except for the controversially large values seen on Ni(111) with $c(4 \times 2)$-2CO structure [28,29].

In the calculations on the Pd(111) surface with three different CO coverages and structures, some changes in the CO bond length have been reported as a function of adsorption site [43]. For the $(\sqrt{3} \times \sqrt{3})R30^\circ$ symmetry the C—O bond lengths are 1.16 Å for top, 1.18 Å for bridge, and 1.19 Å for fcc and hcp sites. For the $c(4 \times 2)$-2CO symmetry the C—O bond lengths are 1.18 Å if both molecules are either at the bridge sites or at the fcc and hcp sites. For the (2×2)-3CO symmetry the values at the top site are around 1.15 Å and the bridge sites or the fcc and hcp sites indicate values around 1.18 Å.

If the error bars in Fig. 3 are taken into account, it seems that the C—O bond length can be regarded as constant as a function of the carbon—substrate bond length or as a function of carbon coordination on the surface given in Eq. (1).

6. Conclusions

In this study we have presented a quantitative structural analysis of the $(\sqrt{3} \times \sqrt{3})R30^\circ$-CO structure on the Co(0001) surface using low-energy electron diffraction together with dynamical LEED calculations. The CO molecules adsorb on the top site perpendicular to the surface with the carbon atom bonding to a Co atom. The CO bond length is 1.17 ± 0.06 Å and the Co—C distance is 1.78 ± 0.06 Å. The first Co layer distance undergoes small buckling where the Co atoms underneath the CO molecule are pulled 0.04 ± 0.04 Å outwards.

Acknowledgements

This work was supported by the Academy of Finland and by the Director, Office of Energy Research, Office of Basic Energy Sciences, Materials Sciences Division of the US Department of Energy under Contract No. DE-AC03-76SF00098. J.L. and K.K. acknowledge the financial support of the Neste Foundations. E.A.S acknowledge CNPq, a Brazilian research agency, for financial support.

References

[1] P.R. Watson, M.A. Van Hove, K. Herman, NIST Surface Structure Database, Ver. 3.0, NIST Standard Reference Data Program, National Institute of Science and Technology, Gaithersburg, 1996.
[2] G. Michalk, W. Moritz, H. Pfnür, D. Menzel, Surf. Sci. 129 (1983) 92.
[3] H. Over, W. Moritz, G. Ertl, Phys. Rev. Lett. 70 (1993) 315.
[4] M. Gierer, A. Barbieri, M.A. Van Hove, G.A. Somorjai, Surf. Sci. 391 (1997) 176.
[5] T. Giessel, O. Schaff, C.J. Hirschmugl, V. Fernandez, K.-M. Schindler, A. Theobald, S. Bao, R. Lindsay, W. Berndt, A.M. Bradshaw, C. Baddeley, A.F. Lee, R.M. Lambert, D.P. Woodruff, Surf. Sci. 406 (1998) 90.
[6] H. Ohtani, M.A. Van Hove, G.A. Somorjai, Surf. Sci. 187 (1987) 372.
[7] D.F. Ogletree, M.A. Van Hove, G.A. Somorjai, Surf. Sci. 173 (1986) 351.
[8] S.D. Kevan, R.F. Davis, D.H. Rosenblatt, J.G. Tobin, M.G. Mason, D.A. Shirley, C.H. Li, S.Y. Tong, Phys. Rev. Lett. 46 (1981) 1629.
[9] E.J. Moler, S.A. Kellar, W.R.A. Huff, Z. Hussain, Phys. Rev. B 54 (1996) 10 862.
[10] M.E. Bridge, C.M. Comrie, R.M. Lambert, Surf. Sci. 67 (1977) 393.
[11] J. Lahtinen, J. Vaari, K. Kauraala, Surf. Sci. 418 (1998) 502.
[12] H. Papp, Surf. Sci. 129 (1983) 205.
[13] F. Greuter, D. Heskett, E.W. Plummer, H.-J. Freund, Phys. Rev. B 27 (1983) 7117.
[14] G. Broden, T.N. Rhodin, C. Bruckner, R. Benbow, Z. Hurych, Surf. Sci. 59 (1976) 593.

[15] R.L. Toomes, D.A. King, Surf. Sci. 349 (1996) 1.
[16] H. Papp, Surf. Sci. 149 (1985) 460.
[17] K.A. Prior, K. Schwaha, R.M. Lambert, Surf. Sci. 77 (1978) 193.
[18] U. Bardi, P. Tiscione, G. Rovida, Appl. Surf. Sci. 127 (1986) 299.
[19] J. Lahtinen, J. Vaari, A. Talo, A. Vehanen, P. Hautojärvi, Vacuum 41 (1990) 112.
[20] T. Vaara, J. Vaari, J. Lahtinen, Surf. Sci. 395 (1998) 88.
[21] J. Lahtinen, J. Vaari, T. Vaara, P. Kaukasoina, M. Lindroos, Surf. Sci. 425 (1999) 90.
[22] J. Vaari, J. Lahtinen, T. Vaara, P. Hautojärvi, Surf. Sci. 346 (1996) 1.
[23] J. Lahtinen, J. Vaari, A. Talo, A. Vehanen, P. Hautojärvi, Surf. Sci. 245 (1991) 244.
[24] J. Vaari, Doctoral Thesis, Helsinki University of Technology, 1995.
[25] B. Narloch, D. Menzel, Surf. Sci. 412–413 (1998) 562.
[26] A. Barbieri, M.A.Van Hove, httl://electron.lbl.gov/software.
[27] J.B. Pendry, J. Phys. C 13 (1980) 937.
[28] R. Davis, R. Toomes, D.P. Woodruff, O. Schaff, V. Fernandez, K.-M. Schindler, K.-U. Weiss, R. Dippel, V. Fritsche, A.M. Bradshaw, Surf. Sci. 393 (1997) 12.
[29] L.D. Mapledoram, M.P. Bessent, A. Wander, D.A. King, Chem. Phys. Lett. 228 (1994) 527.
[30] Ph. Hoffmann, K.-M. Schindler, S. Bao, V. Fritzsche, A.M. Bradshaw, D.P. Woodruff, Surf. Sci. 337 (1995) 169.
[31] D.J. Hannaman, M.A. Passler, Surf. Sci. 203 (1988) 449.
[32] Z.Q. Huang, Z. Hussain, W.T. Huff, E.J. Moler, D.A. Shirley, Phys. Rev. B 48 (1993) 1096.
[33] C. Zhao, M.A. Passler, Surf. Sci. 320 (1994) 1.
[34] J.D. Batteas, A. Barbieri, E.K. Starkey, M.A. Van Hove, G.A. Somorjai, Surf. Sci. 313 (1994) 341.
[35] S. Andersson, J.P. Pendry, J. Phys. C 13 (1980) 3547.
[36] M. Passler, A. Ignatiev, F. Jona, D.W. Jepsen, P.M. Marcus, Phys. Rev. Lett. 43 (1979) 360.
[37] S.Y. Tong, A. Maldonado, C.H. Li, M.A. Van Hove, Surf. Sci. 94 (1980) 73.
[38] C.F. McConville, D.P. Woodruff, K.C. Prince, G. Paolucci, V. Chab, M. Surman, A.M. Bradshaw, Surf. Sci. 166 (1986) 221.
[39] R.J. Behm, K. Christmann, G. Ertl, M.A. Van Hove, J. Chem. Phys. 73 (1980) 2984.
[40] B.E. Hayden, A.M. Bradshaw, Surf. Sci. 125 (1983) 787.
[41] M. Kawai, J. Yoshinobu, Surf. Sci. 368 (1996) 239.
[42] A.P. Seitsonen, Doctoral Thesis, Berlin University of Technology, 1999.
[43] D. Loffreda, D. Simon, P. Sautet, Surf. Sci. 425 (1999) 68.
[44] R. Ramprasad, K.M. Glassford, J.B. Adams, R.I. Masel, Surf. Sci. 360 (1996) 31.
[45] A. Beutler, E. Lundgren, R. Nyholm, J.N. Andersen, B.J. Setlik, D. Heskett, Surf. Sci. 396 (1998) 117.
[46] J.J.C. Geerlings, M.C. Zonnevylle, C.P.M. de Groot, Surf. Sci. 241 (1991) 315.
[47] N. Materer, A. Barbieri, U. Starke, J.D. Batteas, M.A. Van Hove, G.A. Somorjai, Phys. Rev. B 48 (1993) 2859.
[48] G. Bihlmayer, R. Eibler, R. Podloucky, Surf. Sci. 402–404 (1998) 794.
[49] Y. Morikawa, J.J. Mortensen, B. Hammer, J.K. Norskov, Surf. Sci. 386 (1997) 67.